

Supplementary Information for

# Contactless manufacturing of TERS-active AFM tips by bipolar electrodeposition

*Yuhan Huang, David Talaga, Gerardo Salinas, Patrick Garrigue, Gary S. Cooney, Stéphane Reculosa, Alexander Kuhn, Sébastien Bonhommeau\* and Laurent Bouffier\**

Univ. Bordeaux, CNRS, Bordeaux INP, ISM, UMR 5255, F-33400 Talence, France.

\*To whom correspondence should be addressed. Emails: [sebastien.bonhommeau@unibordeaux.fr](mailto:sebastien.bonhommeau@unibordeaux.fr), [laurent.bouffier@cnrs.fr](mailto:laurent.bouffier@cnrs.fr)

## Table of Contents

Possible electrochemical reactions during the bipolar electrodeposition (Table S1) .....	3
Plating solution concentration .....	3
Variation of gold thickness during the bipolar electrodeposition (Tables S2) .....	3
EDX analysis of TERS tips (Figure S1) .....	4
Parallel fabrication of three TERS tips (Table S3) .....	5
Fabrication of TERS tips at different electric potentials (Figure S2) .....	5
TERS point measurements using three additional tips (Figure S3) .....	6
TERS maps from two additional tips (Figures S4 and S5) .....	7
Unmagnified AFM images of GO flake in Figure 3 and 4 (Figure S6) .....	8
Picture of the Electrochemical Cell (Figure S7) .....	8
Analysis of Standard Errors of Deposited TERS Tips ROC (Figure S8).....	9

## Possible electrochemical reactions during the bipolar electrodeposition

**Table S1.** Standard potentials for redox couples involved in the bipolar electrodeposition

Electrochemical reaction	Standard potential /V vs. SHE*
$O_2(g) + 4H^+ + 4e^- \rightleftharpoons 2H_2O$	+1.23
$[Au(SO_3)_2]^{3-} + e^- \rightleftharpoons Au(s) + 2SO_3^{2-}$	+0.77
$SiO_2 + 4H^+ + 4e^- \rightleftharpoons Si + 4H_2O$	-0.91

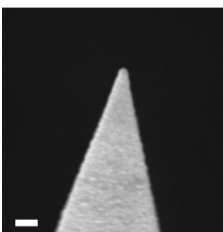
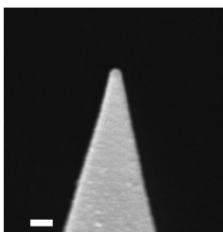
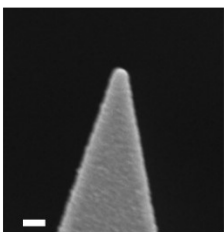
\*Standard Hydrogen Electrode

### Plating solution concentration

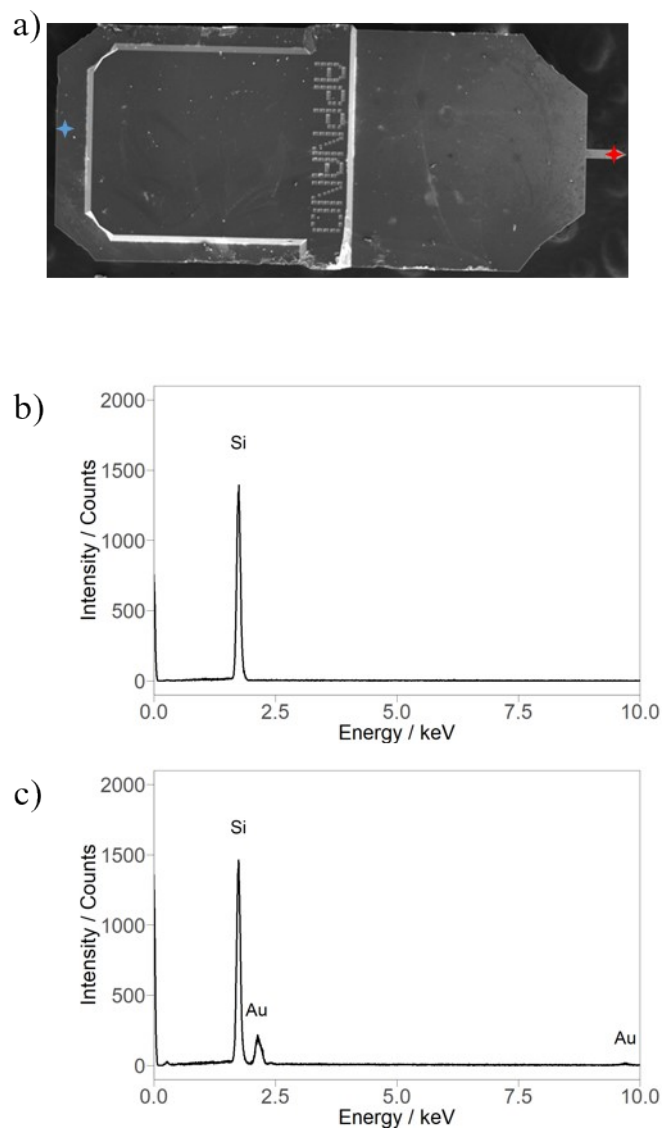
The gold precursor concentration in the plating solution is 10 g/L, as indicated by the supplier Metalor. It is observed that after using the plating solution for 2-3 times, no significant effect on the thickness or distribution of the deposited gold layers. This might contribute to the minimal consumption of gold during the electrochemical process, and the high concentration of the plating solution. As the commercial plating solution is optimized with proprietary additives that promote smooth and uniform gold deposition, simple dilution would not only reduce the concentration of the gold precursor but it would also decrease the concentration of these essential additives, potentially impacting the quality of the gold layer. Therefore, the original concentration of the solution was maintained for consistent and high-quality deposition, and no study as a function of the concentration was achieved.

### Variation of gold thickness during the bipolar electrodeposition

**Table S2.** Variation of gold thickness as a function of the electrodeposition time for a 6.9 V/cm electric field (-11 V applied voltage).

Exp. Conditions: Applied voltage Electrodeposition time	-11 V 5 s	-11 V 10 s	-11 V 15 s
SEM image Scale bar 500 nm			
Radius of curvature (ROC)	ROC ~90 nm	ROC ~135 nm	ROC ~180 nm

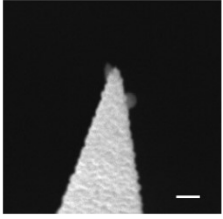
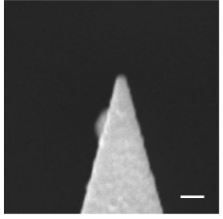
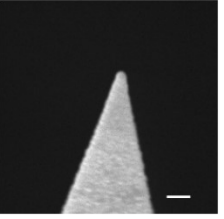
## EDX analysis of TERS tips



**Figure S1.** **a)** SEM image of a representative chip after Au electrodeposition (fabrication parameters: 6.9 V/cm electric field, 5 s electrodeposition time) with the localization of points where the energy dispersive X-ray (EDX) analysis has been performed (blue and red stars, respectively). **(b)** EDX analysis collected on the blue star (i.e. the cathodic pole where no electrodeposition occurred) and **(c)** on the red star (i.e. the anodic pole where gold electrodeposition took place).

## Parallel fabrication of three TERS tips

**Table S3.** Results of gold thickness of three AFM tips after Au electrodeposition. The three tips were fabricated in the same batch for a 6.9 V/cm electric field (-11 V applied voltage). The SEM images were taken after TERS testing on GO sample. The bump-like structures observed in the vicinity of TERS tip apexes in the first two SEM images should be a contaminant, which adsorbed onto the tip during TERS measurements, but not a gold defect since their brightness is not consistent with gold. Optical video images used during tip-laser alignment and SEM measurements confirm that these structures were absent before TERS experiments, and were not observed on any freshly-fabricated TERS tips that had not undergone TERS measurements.

Exp. Conditions: Applied voltage Electrodeposition time	-11 V 5 s	-11 V 5 s	-11 V 5 s
SEM image Scale bar 500 nm			
Radius of curvature (ROC)	ROC ~87 nm	ROC ~90 nm	ROC ~85 nm

## Fabrication of TERS tips at different electric potentials

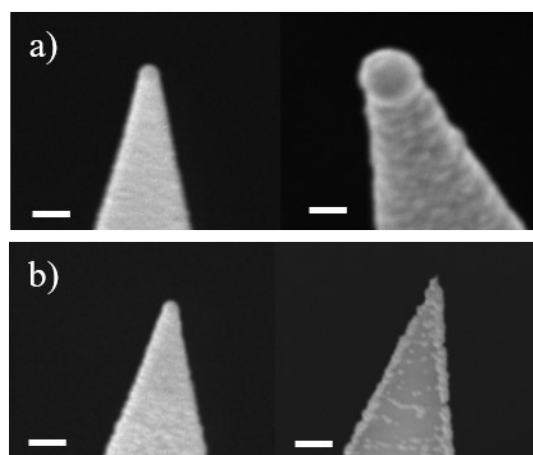


**Figure S2.** SEM images of two AFM tips after Au electrodeposition with different fabrication parameters: a) left: 6.9 V/cm electric field and 10 s electrodeposition time, right: 7.5 V/cm electric field and 10 s electrodeposition time; b) left: 6.9 V/cm electric field and 5 s electrodeposition time, right: 6.3 V/cm electric field and 5 s electrodeposition time. Scale bars: 500 nm. In Figure S2a, the ROC is 135 nm (left) and 385 nm (right). In Figure S2b, the ROC is 90 nm (left) and 60 nm (right). Using 6.3 V/cm for 5 s, a homogeneous gold film was not formed.

## TERS point measurements using three additional tips

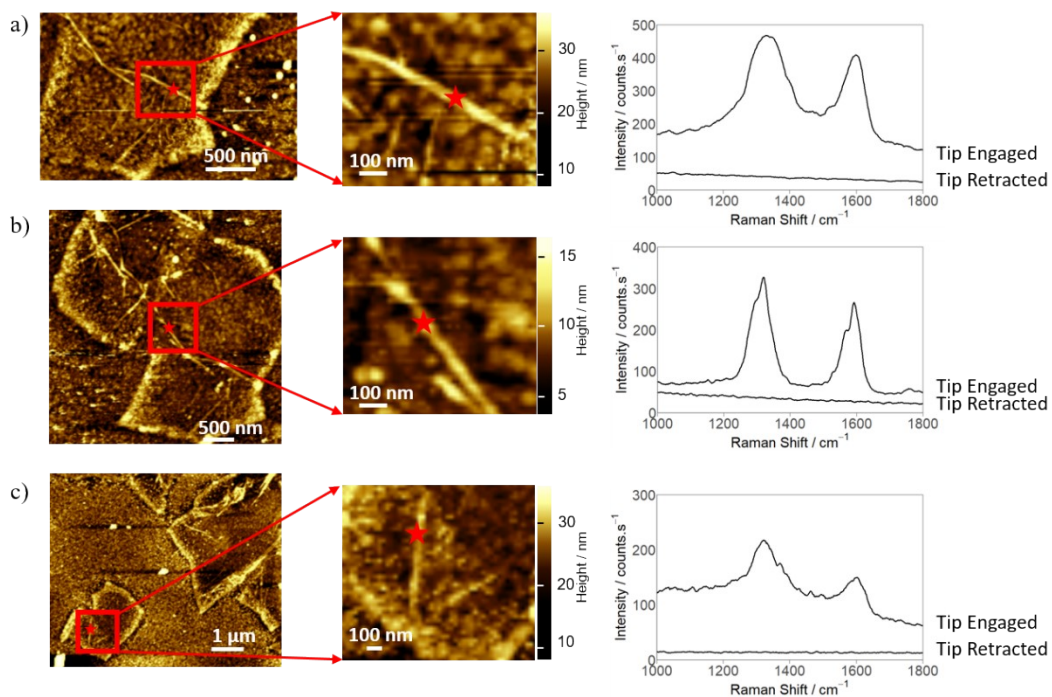


**Figure S3.** Tapping-mode topographic AFM image at the edge of a GO flake, and corresponding TERS spectra obtained using three different TERS tips (fabrication parameters: 6.9 V/cm electric field, 5 s electrodeposition time). Red squares in the AFM images correspond to the zoom-in area and red stars in the indicate points correspond to TERS spectra.

## TERS maps from two additional tips

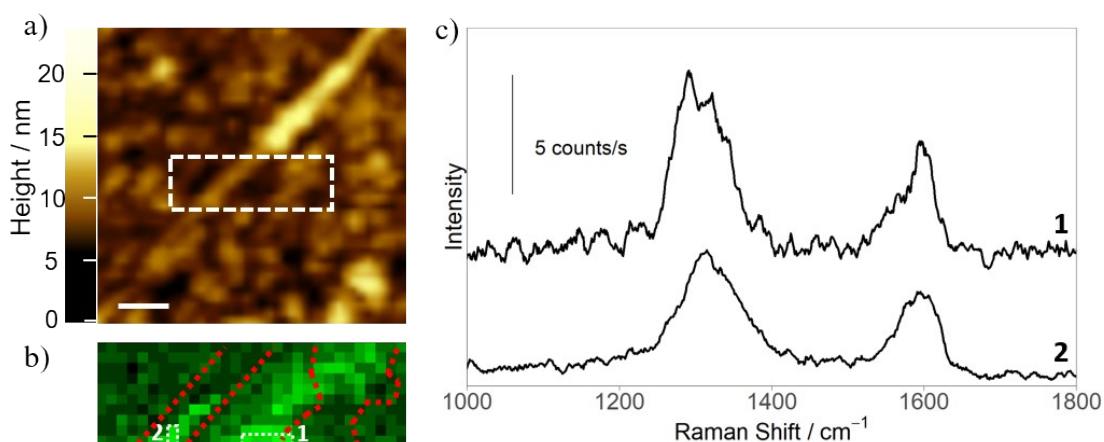


**Figure S4.** (a) Tapping-mode topographic AFM image at the edge of a GO flake. The red dotted lines indicate the edge of a GO flake within a multilayer structure. Scale bar: 100 nm. (b) TERS map bounded by the white dotted rectangular box in Figure S4a. It is obtained by intensity integration in the spectral range spanning from  $1230\text{ cm}^{-1}$  to  $1650\text{ cm}^{-1}$ . Scanning step size: 10 nm, acquisition time: 3 s. (c) TERS spectra 1 and 2 correspond to the mean spectra averaged over areas bounded by the white dotted rectangle boxes in Figure S4b.

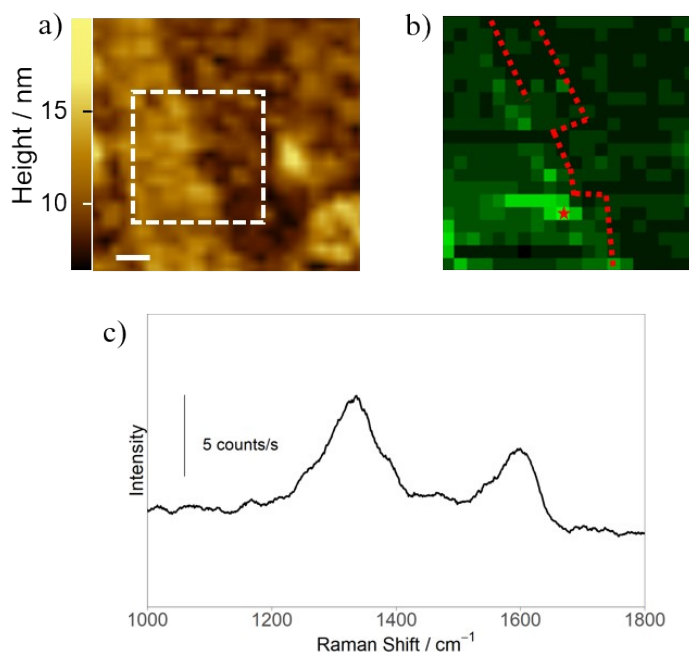


**Figure S5.** (a) Tapping-mode topographic AFM image at the edge of a GO flake. Scale bar: 100 nm. (b) TERS map bounded by the white dotted square box in Figure S5a, obtained by intensity integration in the spectral range spanning from  $1230\text{ cm}^{-1}$  to  $1650\text{ cm}^{-1}$ . The red dotted lines indicate the edge of a GO flake within a multilayer structure. Scanning step size: 20 nm, acquisition time: 5 s. (c) TERS spectrum extracted from the pixel marked with a red star in Figure S5b.

## Unmagnified AFM images of GO flake in Figure 3 and 4

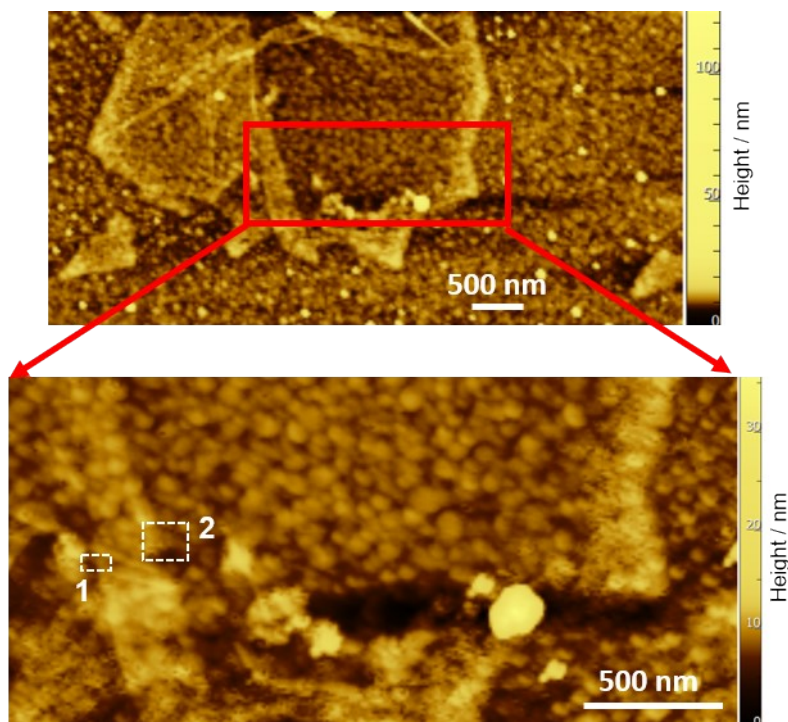


**Figure S6.** Tapping-mode topographic AFM image showing part of a GO flake. The top image shows a larger area of the GO flake, while the bottom image is an enlarged section of the area highlighted with red square. The white dashed squares labeled 1 and 2 correspond to the TERS imaging areas shown in Figure 3.

## Picture of the Electrochemical Cell

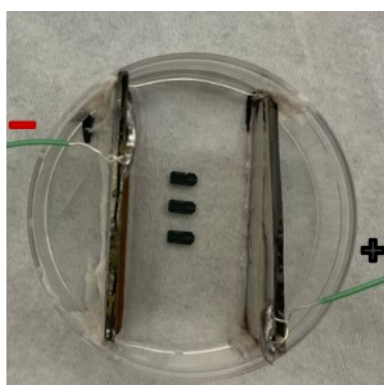


**Figure S7.** Top view of the electrochemical cell used for Au electrodeposition. Three AFM chips are immersed in the plating solution, placed parallel to each other and perpendicular to the feeder electrodes, with tip apex facing the feeder anode.



## Analysis of Standard Errors of Deposited TERS Tips ROC

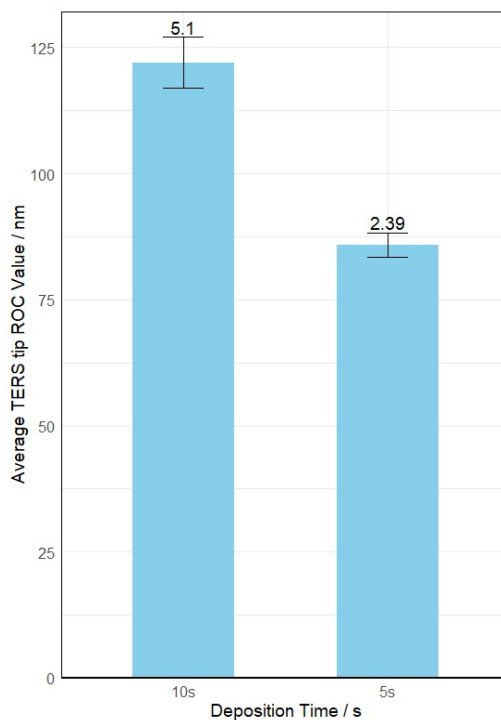


**Figure S8.** Average ROC values for deposited tips at two different deposition time (10 s and 5 s) under the same 6.9 V/cm electric field (-11 V applied voltage). Error bars indicate the standard error (SE) of the ROC value of the tips, with a SE value of 5.1 for tips coated during 10 s (5 tips in total) and 2.39 for tips coated during 5 s (8 tips in total). These results show that both deposition time produced reliable results, the 10 s deposition time showed a bigger degree of variability.